

DESIGN OF ACTIVE CONTROLS FOR THE NASA

F-8 DIGITAL FLY-BY-WIRE AIRPLANE

Joseph Gera
Langley Research Center

SUMMARY

This paper describes the design of a set of control laws for the NASA F-8 digital fly-by-wire research airplane. These control laws implement several active controls functions: maneuver load control, ride smoothing and departure-boundary limiting. Included in the description are the criteria and methods which were used in the design of the control laws. Results of linear analyses and nonlinear simulation are summarized in the paper.

INTRODUCTION

The National Aeronautics and Space Administration has been conducting research in digital fly-by-wire technology. In the initial phase of this research program an Apollo Lunar Module computer and inertial measuring unit were installed in an F-8C airplane. Flight tests were conducted on this airplane at the Dryden Flight Research Center with the mechanical control links removed for the very first flight. These tests demonstrated the feasibility of digital fly-by-wire controls for conventional airplanes and the fact that such systems can incorporate sufficient reliability for pilot confidence (ref. 1). The second or current phase of the program is directed at (1) demonstrating flight control systems using multiple redundant general-purpose digital computers with redundant sensors and actuators and (2) flight testing of those control laws which have become feasible only with the increased speed and memory of current airborne digital computers.

The first set of control laws selected for flight testing has been designed. It includes several functions which are projected for use in future active controls applications. Some of these functions have been flight-tested individually in the past; in the present program they are integrated into a single, full-authority, flight-critical control system. This paper describes the design criteria and methods used in developing the control laws. The discussion also includes simulation experience with the control laws.

SYMBOLS

All units of measurements are as given below except where noted otherwise.

C_1, C_2	constants (eq. (1))
C^*	response variable, g units
$f_i, i=1, \dots, n$	functions used in gain scheduling
g	gravitational acceleration, m/sec ²
h	altitude, m
$K_i, i=1, \dots, n$	gain
K_{C^*}	CAS forward loop gain, deg/g
K_{XF}	symmetric aileron-to-elevator gain, deg/deg
M	Mach number
N_z	normal acceleration, g units
q	pitching velocity, rad/sec
V_{co}	'cross-over' velocity, m/sec
z	forward-difference operator (e.g., $z(q) = q_{n+1}$)
α	angle of attack, deg
α_L	envelope limit, deg
α_{TRIM}	trim angle of attack, deg
β	angle of sideslip, deg
ω_n	undamped natural frequency, rad/sec
ω_{sp}	frequency of longitudinal short period motion, rad/sec
ζ	damping ratio

ζ_{sp} damping ratio of short period motion

Abbreviations:

CAS command augmentation system
SAS stability augmentation system

DISCUSSION

Modeling

In any control law design one of the most important factors is the mathematical model of the controlled vehicle. The complete design cycle made use of two distinct models of the F-8 airplane. The first of these is a complete, nonlinear representation of the rigid F-8 airplane, flexibility effects, control surface actuation system and the flight environment (ref. 2). From the complete representation the linearized equations of motion were obtained by numerical differentiation after trimming the airplane at various altitudes, Mach numbers, fuel loads and load factors. The resulting set of linear equations of motion covered the entire operational envelope of the F-8 airplane including some high angle of attack conditions where the lateral-directional stability characteristics of the basic airplane required considerable improvement. Most of the aerodynamic data used in the mathematical model was already available except for the symmetric aileron effectiveness at high subsonic speeds. The latter became the subject of a short wind tunnel investigation using an existing model of the F-8C.

Control Law Design

Each of the pitch, roll and yaw axes have several pilot selectable control modes. The modes for the pitch axis are:

- (a) Direct mode, which is essentially a proportional control mode between the pilot's stick and the horizontal tail.
- (b) SAS mode. This mode was designed to improve the damping of the short period motion by compensated pitch rate feedback to the horizontal tail.
- (c) CAS mode. This mode was designed to incorporate several active controls functions. These functions will be defined and briefly described in this section.

For further design details the reader is referred to reference 3. The modes for the lateral and directional axes are:

- (a) Direct modes for the roll and yaw axes which are similar in structure to the pitch direct mode.

(b) SAS modes for the roll and yaw axes which will be described later.

Conventional autopilot functions are also provided when the roll and yaw SAS modes and the pitch CAS mode are engaged.

Pitch CAS Mode.— This mode implements several active control functions. The term 'active control' means that the control system design is an integral part of a new airplane configuration development task. Since no aerodynamic or structural modifications have been made to the F-8 in the digital fly-by-wire program, flight testing the active control functions will not reveal the full performance benefits achievable by active controls. Instead, the flight tests will be aimed at evaluating the mutual interactions of the various active control concepts.

Figure 1 illustrates the basic CAS mode in the pitch axis augmentation system. In the basic CAS mode the shaped pilot's stick deflection controls a blend of pitching velocity and normal acceleration. The resulting signal is routed to the actuation system via the variable gain, K_{C^*} . The latter is a function of dynamic pressure derived from altitude and Mach number. In order to minimize stick forces resulting from changing trim conditions, neutral speed stability is provided by an effective forward loop integration. The integration itself is accomplished by cancelling the position feedback signal of the elevator secondary actuators at low frequencies. The mechanical output of the secondary actuators is then used to drive the primary or power actuators which are connected directly to the control surfaces.

A significant feature of this control law is that it was designed through the application of linear optimal control theory at selected flight conditions. Specifically, the motion variable, C^* defined as

$$C^* = N_z + \frac{V}{g} q$$

was compared with the output of a linear, second-order 'command' model ($\omega_n = 7.4$ rad/sec; $\zeta = .91$). Minimization of a cost functional consisting of the integral of the weighted squares of the C^* error, its integral, the elevator rate and elevator command resulted in a control law which is a linear combination of the assumed state variables. The control law was simplified by neglecting low-gain loop closures and effecting possible pole-zero cancellations. Additional details of the design procedure are given in reference 3.

The design specifications for the control system included the requirement of limiting the operating envelope of the airplane. Envelope limiting is important for two reasons, the first being that with envelope limiting the pilot can demand the full maneuvering capability of the airplane without

concern for departing from controllable flight. The second reason is that future active control applications will include relaxing the static stability requirements of the basic airplane: elevator commands beyond the available surface authority would result in loss of control for an airplane without envelope limiting.

The implementation of the envelope limiter is shown in figure 2; this system was integrated with the basic C* controller by the use of a switch labeled as 'max. value select.' in figure 1. The switch simply selects the more positive, i.e., the larger nosedown elevator command. It should be noted that at low frequencies the command signal from both controllers approximates elevator rate; switching on this approximate elevator rate has proved to be a satisfactory method to effect transition between the two controllers.

The design of the envelope limiting control law was also accomplished by using linear optimal control theory. In the cost functional the pitching velocity term was heavily weighted along with angle of attack, its integral, elevator rate, and elevator command. The control law obtained at selected flight conditions by using optimal control theory was simplified in a manner similar to simplification of the basic C* controller. The resulting controller is driven by angle of attack and its approximate time derivative obtained by high-passing the pitching velocity. The angle of attack is referenced to the value, α_L , the limit angle of attack. At present α_L is programmed to include the effect of sideslip as

$$\alpha_L = C_1 - C_2 |\beta| \tag{1}$$

where C_1 and C_2 are constants.

Direct lift produced by symmetric aileron or flap deflections is utilized both for drag reduction in maneuvering flight and for ride smoothing in turbulence. The direct lift mode has the complementary structure illustrated in figure 3. Reduction of maneuvering drag is accomplished by scheduling steady state flap deflections with lagged pitching velocity. For ride smoothing the measured normal acceleration is fed back to the flaps via a scheduled gain and a high-pass filter. Tentative values of the scheduled gain were derived from loop gain considerations (ref. 3). The use of the high-pass filter avoids the necessity of gravity compensation of the accelerometer signal during steady climbs or descents. Pitching moment changes due to flap deflection are canceled by utilizing a cross-feed signal through the gain K_{XF} which is chosen to be the ratio of pitching moments produced by unit deflections of the elevator and of the flaps.

Roll SAS and Yaw SAS Modes.— Figure 4 illustrates the mechanization of the augmented modes for the lateral-directional axes. Although the roll SAS and yaw SAS modes are individually selectable by the pilot, this discussion treats

them collectively. The criteria for the design of this system included improved damping of the Dutch roll oscillating mode, positive directional stability and good turn coordination at all usable angles of attack. Application of the linear quadratic optimal control algorithm at selected flight conditions yielded a feedback gain matrix with a non-zero gain on every state variable to every control input. A separate algorithm, described in reference 4, was then used to drive those gains to zero which were impractical to implement while still satisfying conditions necessary to minimize the original cost function. In the resulting control mode, high-passed yaw rate provides improved Dutch roll damping with no steady state turn resistance. Turn coordination is enhanced by compensated lateral acceleration feedback and aileron-rudder interconnect. Automatic rudder trim is achieved by the feedback of integrated lateral acceleration to the rudder. The latter loop is opened whenever the rudder pedals are out of detent, thus enabling the pilot to command a steady sideslip. The scheduling of gains is done with angle of attack to ensure good performance at all maneuvering conditions.

Autopilot Functions.- Conventional autopilot functions are available to the pilot in addition to the inner loop functions described above. These functions are the following: attitude, altitude, Mach and heading hold modes; control stick steering and heading select are also provided with automatic return to the hold modes.

Digital Processing of Control Laws.- In order to be processed by a digital computer, the control laws must be expressed in the form of difference equations. When the equations of motion of the controlled system are converted to difference equations at the outset, finding the solution of the resulting discrete linear optimal control problem leads directly to control laws which are in the form of difference equations. These control laws are optimal relative to the particular sampling interval chosen at the beginning of the design. Changing the sampling interval requires a new design. If the control law design proceeds in the continuous time domain at the beginning and the resulting continuous control laws are then converted into difference equations, a new sampling interval does not usually require solving the entire optimal control problem again. For a limited range of sampling intervals all that is required is recomputing the coefficients of the linear difference equations expressing the control laws. The latter approach of obtaining difference equations is directly applicable to control laws which are designed for multi-rate sampling.

The difference equations which are programmed in the F-8 flight computers were obtained by the second method. Thus it will be possible to study the effects of different sampling intervals in flight by a simple preflight change in the software executive timing routine, after the computer memory has been reloaded with the new coefficients of the difference equations. These coefficients are calculated from the continuous control laws off-line using Tustin's method (ref. 5). Initially, all inner loop control law functions are computed at 20 millisecond intervals while the autopilot functions and other less critical operations are executed at 80 millisecond intervals.

PERFORMANCE AND SIMULATION RESULTS

Control law performance in the various modes, predicted by linear analysis, was evaluated over the entire flight envelope in closed-loop simulation. Although the basic F-8 airplane has good response characteristics further improvements are expected in the augmented modes.

Longitudinal Modes

In figure 5 longitudinal response is illustrated in the DIRECT, basic CAS and CAS with the direct lift mode at one of the twenty flight conditions used in the design and analysis. Linear analysis gave the following modal characteristics for the short period motion:

	ω_{sp} , rad/sec	ζ_{sp}
DIRECT	3.2	.38
CAS	4.4	.73

Comparing the time histories in these modes in figure 5 shows that these improvements are realized in the full, non-linear simulation. The beneficial effect of the direct lift is reflected in the quickened normal acceleration response with moderately reduced over-shoot in pitch rate.

In figure 6 the role of the symmetric aileron deflection as a ride-smoothing device is shown. The gust-induced normal acceleration traces obtained in the full non-linear simulation substantiate the predictions of linear analysis.

The operation of the envelope limiter was also tested in the simulator. The time histories shown in figure 7 were obtained while the pilot was steadily increasing the load factor in a turning maneuver by applying aft stick pressure. In this particular test the value of α_L was set at a conservative 12 degrees with no contribution from the sideslip term in equation (1). It can be seen that after encountering the angle of attack limit of 12 degrees, any further aft movement of the stick has no effect on the maneuver. Reducing aft stick pressure results in the angle of attack moving smoothly away from the limiting 12 degree value.

Lateral-Directional Modes

Substantial improvements in the lateral-directional response are expected in the combined roll and yaw SAS mode. Linear analysis predicts the following improvements for the Dutch roll mode at the same flight condition ($M = .8$, $h = 6100m$) for which the longitudinal results were presented:

	ω_n , rad/sec	ζ
DIRECT	3.5	.11
SAS (roll and yaw)	3.4	.41

In figure 8 simulator results are shown following a β -gust of two degrees. In the same figure the time histories in response to a step lateral-stick input show the expected improvements in roll-induced sideslip and turn coordination. The latter result was obtained at the same altitude, but reduced airspeed ($M = .4$) which resulted in a moderately high trim angle of attack of 8.9 degrees.

In addition to being the subject of the linear analyses and non-linear simulations, the control law modes were integrated into a single FORTRAN-coded subroutine. The latter was called 32 times per second by the complete F-8 simulation program in a real-time operation. This allowed an early examination of the functional operation of all control modes, mode transfer logic and various initialization routines. This same program was interfaced with an F-8 cockpit and used in preliminary piloted simulations. The subject pilots rated the control law modes favorably, but only the actual flight tests will reveal the benefits of the various active control modes.

CONCLUDING REMARKS

One of the important technology areas the NASA digital fly-by-wire program addresses is the design and flight test of control laws suitable for future active control applications. This report describes a set of control laws, including design criteria and methods, which have been selected for flight tests on the F-8 digital fly-by-wire airplane. The following functions are mechanized in an integrated, full-authority, flight-critical control system:

- (1) Command augmentation system for the pitch axis based on the C^* response criterion, including apparent neutral speed stability.
- (2) Maneuver load control and ride smoothing using direct lift generated by symmetric aileron deflection.
- (3) Envelope limiting which allows the pilot full maneuvering capability without concern for departure from controllable flight regimes.
- (4) Lateral-directional stability augmentation which provides good handling characteristics at all usable angles of attack.

- (5) Conventional autopilot or outer loop functions such as attitude, Mach, altitude and heading hold including control stick steering in these modes.

Linear analyses and non-linear simulation results of the augmented modes predict substantial improvements in the airplane's response characteristics. Pilot comments on these modes have also been favorable, but only the actual flight tests will reveal the extent of benefits achievable by these control modes.

REFERENCES

1. Description and Flight Test Results of the NASA F-8 Digital Fly-By-Wire Control System. NASA TN D-7843, 1975.
2. Woolley, C. T.: A Real-Time Hybrid Simulation of a Digital Fly-By-Wire Aircraft. 1974 Summer Computer Simulation Conference, Houston, TX, July 9-11, 1974.
3. Hartmann, G. L.; Hauge, J. A.; and Hendrick, R. C.: F-8C Digital CCV Flight Control Laws. NASA CR-2629, Feb. 1976.
4. VanDierendonck, A. J.: Design Method for Fully Augmented Systems for Variable Flight Conditions. AFFDL-TR-71-162, January 1972.
5. Fryer, W. D., and Schultz, W. C.: A Survey of Methods for Digital Simulation of Control Systems. Cornell Aeronautical Laboratory Report No. XA-1681-E-1. July 1964.

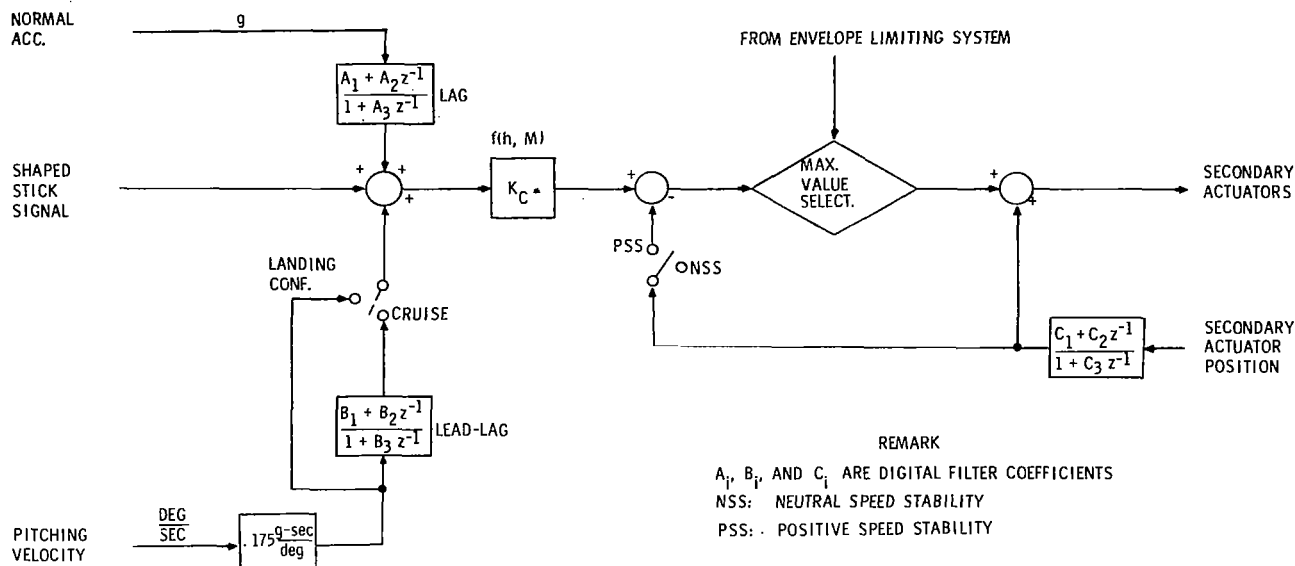


Figure 1.- Basic CAS mode (pitch axis command augmentation system).

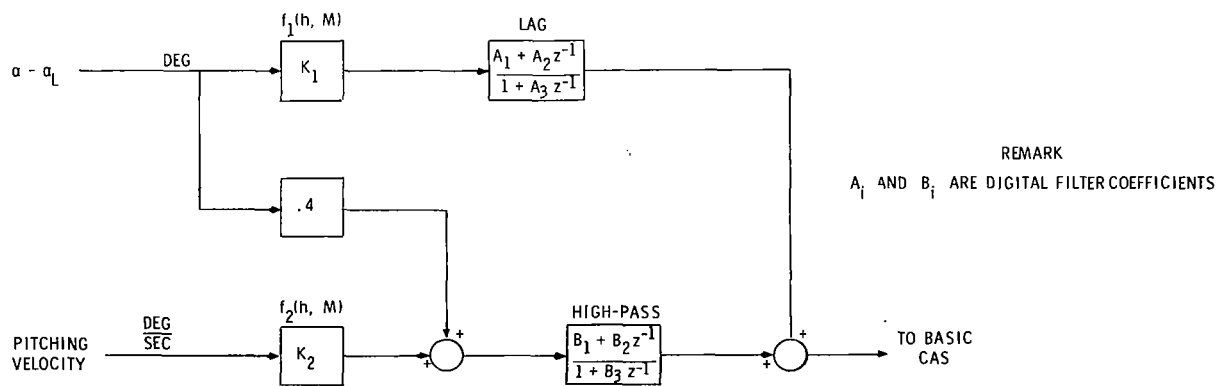


Figure 2.- Envelope limiting system.

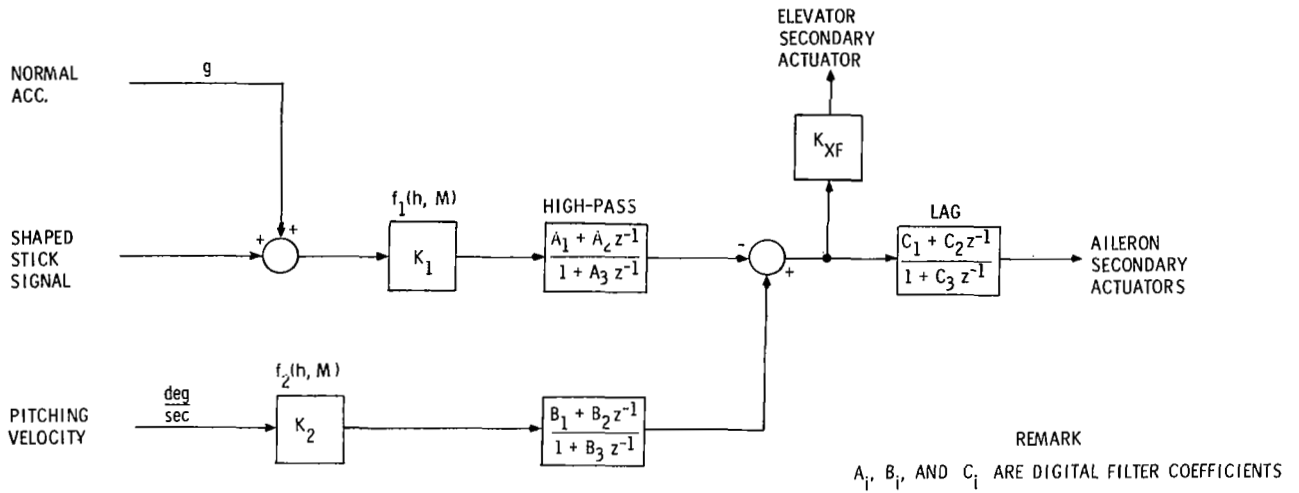


Figure 3.- Maneuver load control and ride-smoothing system.

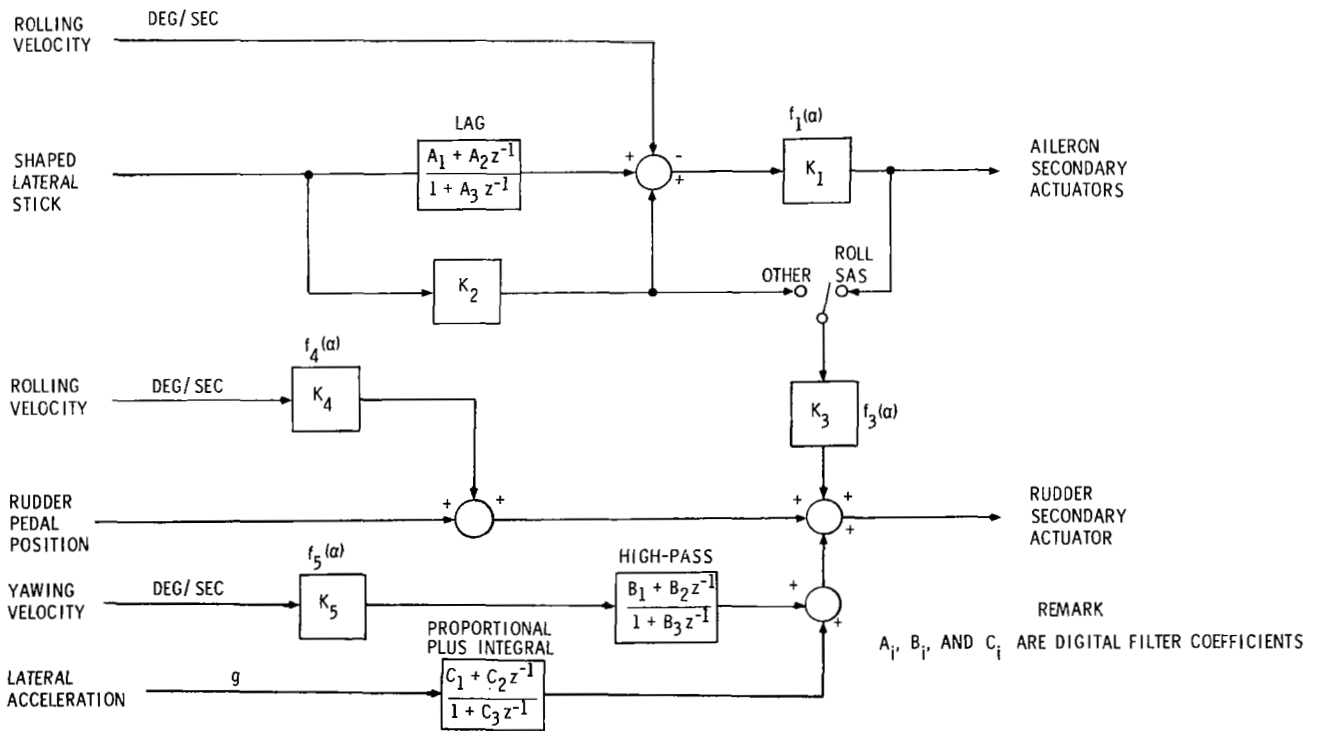


Figure 4.- Lateral-directional stability augmentation system.

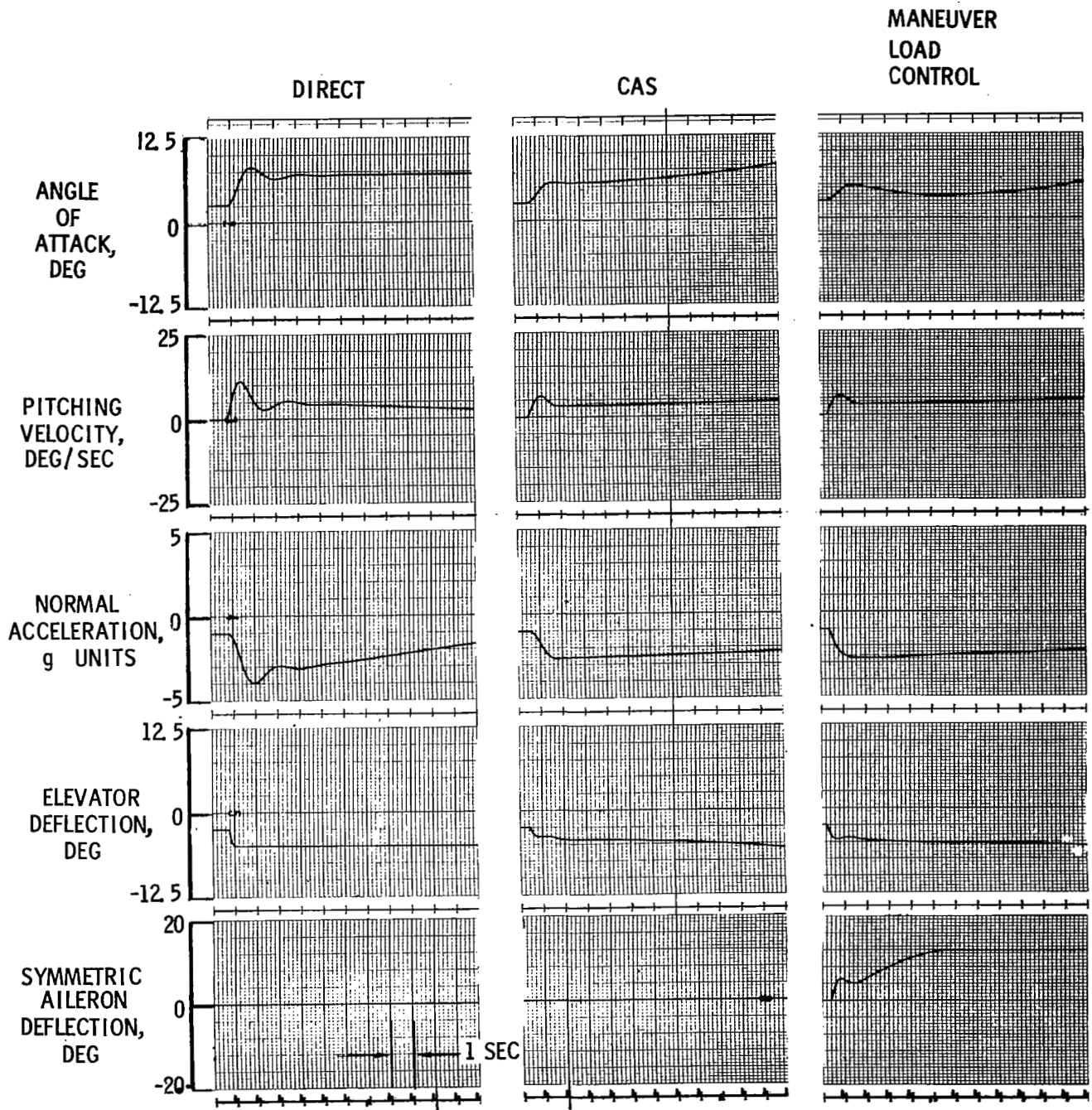


Figure 5.- Longitudinal response to a step stick input. $h = 6100 \text{ m}$; $M = 0.8$.

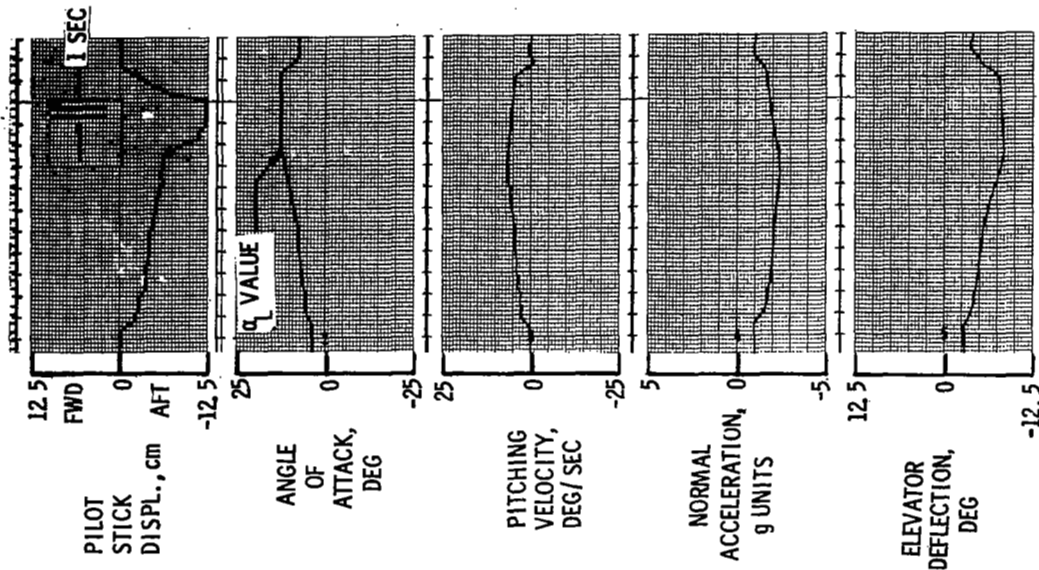


Figure 7.- Envelope limiting in non-linear simulator. $\alpha_{trim} = 3.45^\circ$; $h = 6100$ m; $M = 0.67$.

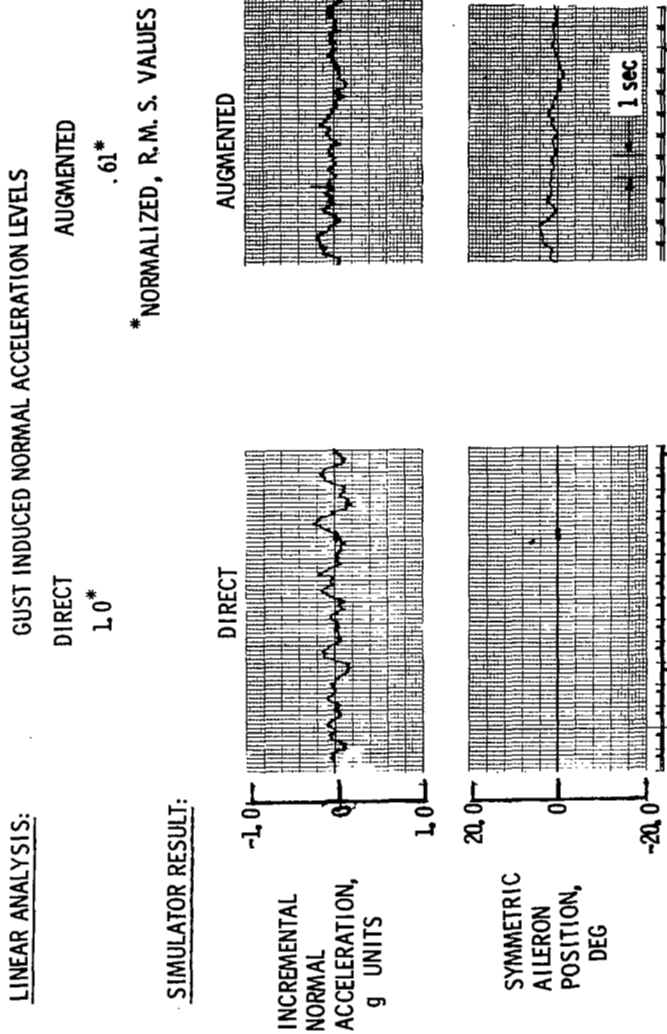


Figure 6.- Predicted performance of ride-smoothing system.

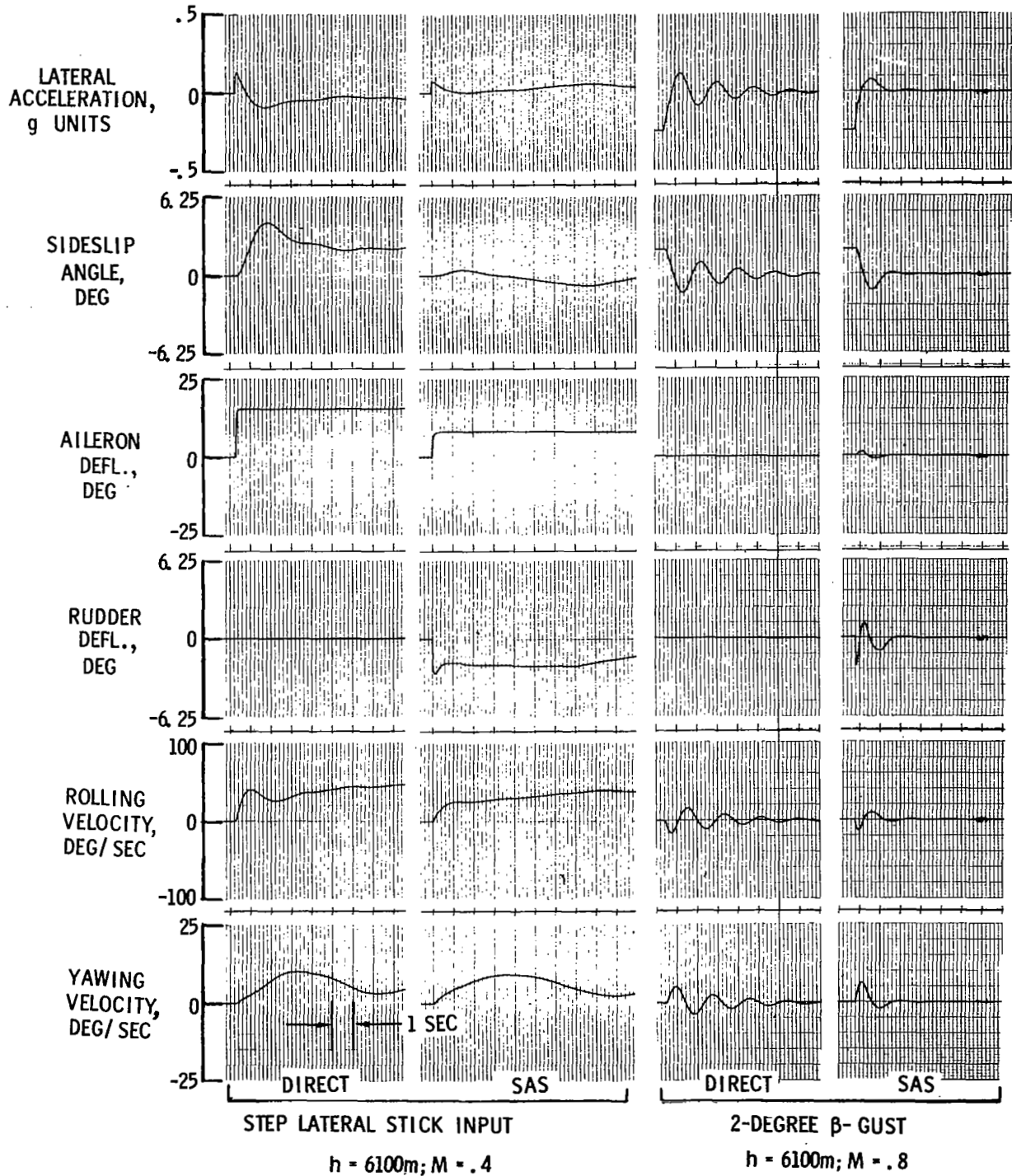


Figure 8.- Lateral-directional response.